Invited Paper

Understanding and Improving Longevity in RF MEMS Capacitive Switches

Chuck Goldsmith*[a], David Forehand[a], Derek Scarbrough[a],
Zheng Peng[b], Cris Palego[b], James Hwang[b], Jason Clevenger[c]
[a]MEMtronics Corp., 3000 Custer Rd. Ste 270-400, Plano, TX, USA 75075;
[b]Lehigh University, 5 East Packard Avenue, Bethlehem, PA USA 18015;
[c]Exponent, 21 Strathmore Road, Natick, MA USA 01760;

ABSTRACT

This paper discusses issues relating to the reliability and methods for employing high-cycle life testing in capacitive RF MEMS switches. In order to investigate dielectric charging, transient current spectroscopy is used to characterize and model the ingress and egress of charges within the switch insulating layer providing an efficient, powerful tool to investigate various insulating materials without constructing actual MEMS switches. Additionally, an in-situ monitoring scheme has been developed to observe the dynamic evolution of switch characteristics during life testing. As an alternative to high-cycle life testing, which may require days or weeks of testing, a method for performing accelerated life tests is presented. Various methods for mitigating dielectric charging are presented including: reduced operating voltage, reduced dielectric area, and improved control waveforms. Charging models, accelerated life test results, and high-cycle life test results for state-of-the-art capacitive RF MEMS switches aid in the better understanding of MEMS switch reliability providing direction for improving materials and mechanical designs to increase the operation lifetime of MEMS capacitive switches.

Keywords: RF MEMS, reliability, dielectric charging, MEMS switches

1. INTRODUCTION

MEMS switch technology has many potential benefits over conventional electronic devices for switching microwave and millimeter-wave signals. MEMS switches possess very low insertion loss, miniscule power consumption, and ultra-high linearity[1]. These characteristics make MEMS technology an ideal candidate for incorporation into passive circuits, such as phase shifters or tunable filters, for implementation in the passive front-end of phased antenna arrays at X-band and above.

With the excellent RF performance of electrostatically-operated, MEMS capacitive switches having been well-established with various component demonstrations, emphasis in RF MEMS research has shifted towards achieving a better understanding of MEMS switch reliability. Efforts have centered on methodologies to quantify the amount of charging present in MEMS capacitive switches, and relating that charging back to the electromechanics of the switch. In this manner, improvements in materials and mechanical designs can be quantified relative to increasing the operational lifetime of MEMS capacitive switches.

The main obstacles to resolving these reliability problems have been two-fold - 1) difficulty in quantifying the amount of charging during switch operation, specifically the ability to characterize and model the ingress and egress of charges in the switch insulator, and 2) lack of in-situ monitoring during life testing, allowing the ability to observe the dynamic evolution of switch characteristics as the switch dielectrically charges towards failure.

This paper discusses the issues relating to reliability and presents methods for performing high cycle life tests of capacitive RF MEMS switches. Measurement and modeling of dielectric charging, as well as monitoring of high-speed and low-speed switching operation provides valuable insight into quantifying the lifetime properties of the switch, and enables estimation of switching lifetime under a variety of operating conditions.

Reliability, Packaging, Testing, and Characterization of MEMS/MOEMS VII, edited by Allyson L. Hartzell,
Rajeshuni Ramesham, Proc. of SPIE Vol. 6884, 688403, (2008) · 0277-786X/08/$18 · doi: 10.1117/12.770586

2. CAPACITIVE SWITCH DESIGN

The switches described in this paper consist of two types of capacitive switches. The first is the traditional RF MEMS capacitive switch with a movable upper membrane and a fixed lower electrode covered by a solid dielectric sheet. An innovative improvement of this switch is the “proximity” or “air-gap” switch, in which most of the dielectric sheet is removed and replaced with dielectric bumps. When the switch is actuated, these bumps keep the upper membrane from touching the lower electrode, but do so with a minimum of dielectric contact. The construction and packaging discussion which follows are appropriate to both types of switches

2.1 MEMS switch construction

Figure 1 is a micrograph of a state-of-the-art metal-dielectric-metal RF MEMS capacitive switch fabricated on a glass substrate. The processes used in the fabrication of this device are similar to those previously reported[1]. The top electrode is a 0.3 μm thick flexible aluminum alloy membrane that is tied to DC and RF ground potential. The bottom switch electrode is composed of chromium/gold and serves as the center conductor of 50 Ω coplanar waveguide for the RF signal. Thick copper posts, approximately 3 μm tall, serve as the anchor points for the suspended MEMS membrane as well as the RF transmission line conductors. Without applied electrostatic force, the membrane is normally suspended in air 2.5 μm above the switch insulator. A control voltage in the range of 25-50 V, applied to the bottom electrode, pulls the membrane into contact with the dielectric thus forming a 120 μm x 80 μm capacitor to shunt the RF signal to ground. When the control voltage is removed, the membrane springs back to its fully suspended position due to the restoring force of the membrane, resulting in little capacitive loading of the RF line.

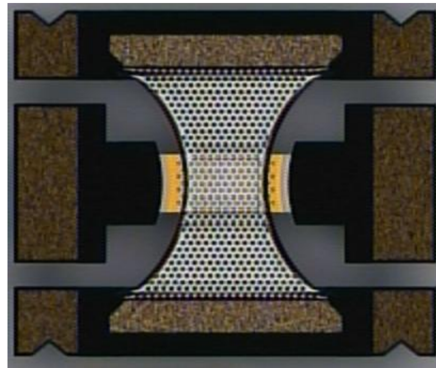

Figure 1 - RF MEMS air-gap switch using patterned dielectric posts.

Within this switch, the layer of switch insulator is composed of sputtered silicon dioxide 0.28 μm thick (εr~4.5). The switch insulator is not a continuous sheet of dielectric, but patterned into a series of insulating, hexagonal posts approximately 4 μm across on an 8 μm pitch. The patterned dielectric bumps create an “air-gap” or “proximity” switch, in which a larger percentage of the switch area utilizes air insulator rather than silicon dioxide. This use of patterned dielectric posts reduces the contact area susceptible to dielectric charging. Trading off on-capacitance for reduced charging provides the opportunity for switching of moderate capacitance ratios (more like a switched reactance than a high isolation switch) with increased switch longevity.

2.2 MEMS switch packaging

Any discussion of MEMS reliability is not complete without clearly defining the environment within which the switch is operating. As such, the packaging of the MEMS switch has a significant impact on its reliability. There are a variety of packaging schemes, most accomplished at the wafer level. Wafer level packaging affords a low-cost packaging paradigm which enables the switch to be packaged while in the confines of a clean, controlled environment (the cleanroom). Most MEMS switch packaging schemes involve either wafer-bonding or microencapsulation. In wafer bonding, a lid wafer is fabricated and bonded to the MEMS substrate, encasing the MEMS switch(s) with a small cavity. In wafer-level microencapsulation, additional sacrificial and structural layers are added to the MEMS device to create a superstructure around the switch, which is then sealed by a liquid encapsulant or chemical vapor deposition. The goal of the packaging is to be as transparent to the RF and reliability characteristics as possible. While the package plays a very important role in determining the environment for switch operation, the package adds to the complexity of understanding the underlying phenomena limiting device reliability. As such, discussion of packaging impact on reliability is beyond

the scope of this article. The characterization and modeling of switch reliability in this article involve the switch, without a package, operated in a clean, dry atmosphere.

3. DIELECTRIC CHARGING

If the environmental causes of MEMS switch failure, such as mechanical contact, excess humidity, contamination, and/or particles are mitigated, then the next cause of failure usually involves the tunneling and trapping of charges within the switch dielectric. This process has been studied by a variety of researchers, attempting to describe the qualitative and quantitative characteristics of charging. At the core of this problem is the fact that when the switch membrane is actuated, it pulls down and comes into contact with the dielectric surface sitting on top of the lower electrode. This dielectric is usually designed for a large capacitance (> 1 pf), often resulting in the dielectric being 1000 – 3000 A thick. With nominal actuation voltages of 25-50 volts, this means that the electric field across the dielectric is on the order of 1-5 MV/cm. At this strong level of electric field, it is possible for charges to tunnel into the dielectric, where they become trapped by the insulating properties of the dielectric. The exact physics of this phenomenon depends of the dielectric composition, deposition conditions, and a variety of other factors. This is, in part, what makes a detailed understanding of dielectric charging so difficult.

Dielectric charging can be grouped into two broad categories. The first type is bottom charging, or bulk charging, of the dielectric. In this case, charges tunnel into the dielectric from the lower switch electrode. Over time, the accumulation of charges into the dielectric from this lower electrode contributes to the electrostatic attraction between the membrane and lower electrode. As such, as more charge accumulates, it takes less and less external voltage to actuate the membrane. The alternative form of charging is top charging, or surface charging. This phenomenon occurs on the top surface of the exposed dielectric, beneath the switch membrane. As charges accumulate on this top surface, they tend to screen the applied voltage, making it harder and harder to pull the membrane down. The action of these two types of dielectric charging is portrayed in Figure 2.

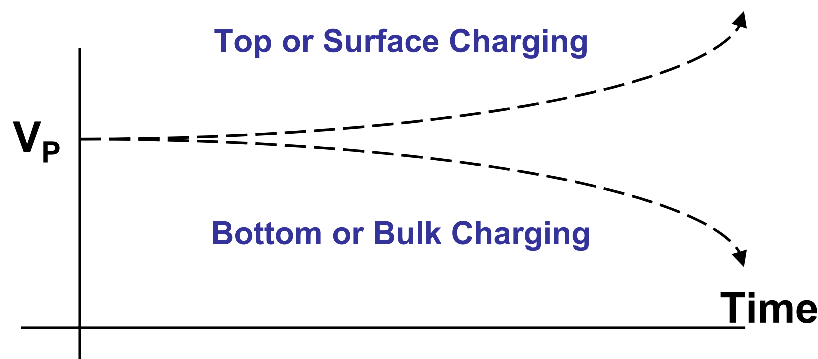

Figure 2 - General behavior of actuation voltage over time in response to surface charging and bulk charging

4. DIELECTRIC CHARGING CHARACTERIZATION

Recently, transient current spectroscopy has been successfully employed to quantify charge tunneling and trapping within a MEMS switch insulator[2]. The references provide in-depth details of the technique, which is summarized here. In transient current spectroscopy, a constant DC voltage is applied to the metal-insulator-metal sandwich of a MEMS switch while high-sensitivity current measurements are made. The polarization charge across the capacitor changes very quickly, with a time constant of pS to nS. However, a much slower charging and discharging phenomena is also observable, and is attributable to the charging of the insulator. Figure 3 depicts the measured charging and discharging current of a capacitive switch structure under 30 volts bias for 250 seconds, then zero bias for 250 seconds. Similar curves are obtained for the negative polarity.

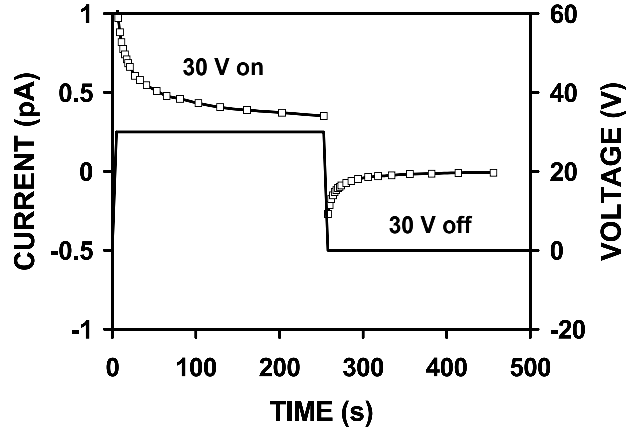

Figure 3 - Measured and modeled current of 30 V charging and discharging current on a permanently down switch. Solid line indicates control voltage.

These currents, measured at varying stress (DC voltage) levels, can then be used to map out the temporal and voltage response of the charges in the switch dielectric. A composite graph of the charging and discharging data at various biases is shown in Figure 4.

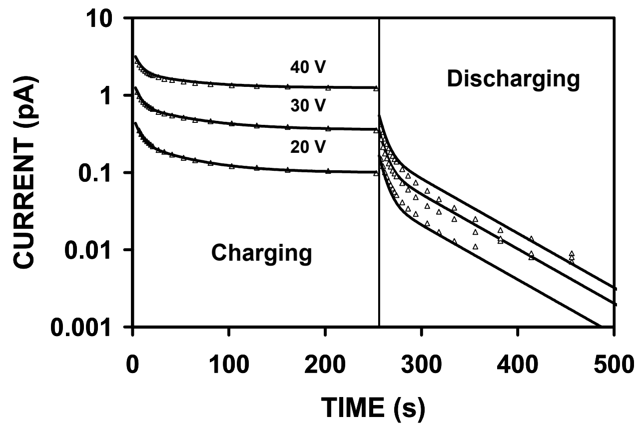

Figure 4 - Modeled and measured (symbols) charging current transients under positive control voltage.

The charging and discharging characteristics of the dielectric can be extracted from these measurements, utilizing a charge model described as

$$Q = \sum_J Q^J [1 - \exp(-t_{ON} / \tau_C^J)] \exp(-t_{OFF} / \tau_D^J), \quad (1)$$

where Q^J is the steady-state charge density of the *Jth* species of trap, τ_C and τ_D are the charging and discharging time constants, t_{ON} and t_{OFF} are the on- and off-times of the switch corresponding to the charging and discharging times. The result is a set of extracted model parameters which describe the charging and discharging time constants, as well as the charge density and voltage dependences of the phenomena. The above data was fitted assuming two carrier species, and resulted in the characterization shown in Table 1.

TABLE I
EXTRACTED MODEL PARAMETERS

Positive Bias				
J	τ_C (s)	τ_D (s)	Q_0 (cm^{-2})	V_0 (V)
1	6.6	6.8	3.1×10^{10}	12.9
2	54.3	61.6	1.6×10^{11}	14.9
Negative Bias				
J	τ_C (s)	τ_D (s)	Q_0 (cm^{-2})	V_0 (V)
1	6.5	7.0	2.4×10^{10}	11.7
2	52.5	74.7	6.0×10^{10}	10.5

\

In order to validate the model, the temporal shift in actuation voltage as a function of DC stress was measured on switches and calculated using the above model. The resulting response shows excellent correlation between measured and modeled voltage shift. Under the controlled set of operating conditions, the model provides an amazingly good approximation to the response of the switch to dielectric charging.

The characterization and modeling techniques presented above have been carried out on both metal-insulator-metal (MIM) capacitors and on MEMS switches fabricated in close proximity to the MIM capacitors. While the charging characteristics of the fixed capacitors does not duplicate the response of the MEMS switches under all conditions (especially in an environment with significant humidity), it does model the switches very well under many practical conditions. This is an extremely powerful tool, in that quick evaluation of various insulating materials are possible without the necessity of fabricating full MEMS switch devices. This evaluation is limited to that of bottom charging of the dielectric. Due to the fixed nature of the MIM capacitors, they are not capable of including surface charging (top charging) that might be present in actual MEMS switches. Top charging usually occurs at higher voltages (> 45 volts) and demonstrates considerably stronger charging (higher charge densities). In addition, top charging usually exhibits very quick charging time constants (~5 sec) and very slow discharging time constants (days or longer). These undesirable characteristics mean that top charging is to be avoided whenever possible.

5. DESIGNING FOR RELIABILITY

The simple and most effective methods for reducing dielectric charging within MEMS switches are to reduce the operating voltage (electric field), reduce the dielectric area, and/or reduce the operating duty cycle[3]. In order to achieve high cycle lifetime, all three of these techniques were utilized to minimize the amount of dielectric charging present within the switch.

5.1 Reduced operating voltage

It has been known for some time that higher operating voltages exponentially decrease the operating lifetime of the switch[4]. The lower limit of operating voltage is determined by the minimum restoring force necessary to ensure that surface forces do not induce stiction of the switch membrane. Further, the minimum control voltage is also determined by the ability to achieve a repeatable tensile stress of the switch membrane during fabrication. Residual stress of aluminum films are dependent on the temperature history of the membrane prior to release. For the equipment set utilized to fabricate these switches, tensile stresses in the 100-150 MPa range are the minimum repeatable values. With the given switch dimensions, this yields switches with approximately 30 volts pull-in voltage.

5.2 Reduced dielectric area

Minimizing the dielectric contact area of MEMS switches is becoming more common as the difficulties of overcoming dielectric charging become evident[5,6]. By changing from a continuous sheet of dielectric beneath the switch to an array of posts, the active area for charging can be reduced. The dielectric posts of 4 μm diameter/8 μm pitch used in this switch has a fill factor of 25%, thereby reducing dielectric charging by 75%. This trades off switch capacitance for reduced charging and increased longevity.

5.3 Improved control waveforms

As discussed above, the applied voltage has a significant impact on switch reliability. In certain cases, where the switch is operated in the on-position for extended periods of time, modification of the control waveform can improve reliability by significant amounts. One method of improving reliability is to utilize a dual-pulse waveform[4], as shown in Figure 5. With this waveform, actuation voltage is only applied for a brief period of time. Afterwards, the control voltage drops to a holding voltage which is above the switch release voltage, but significantly lower than the actuation voltage.

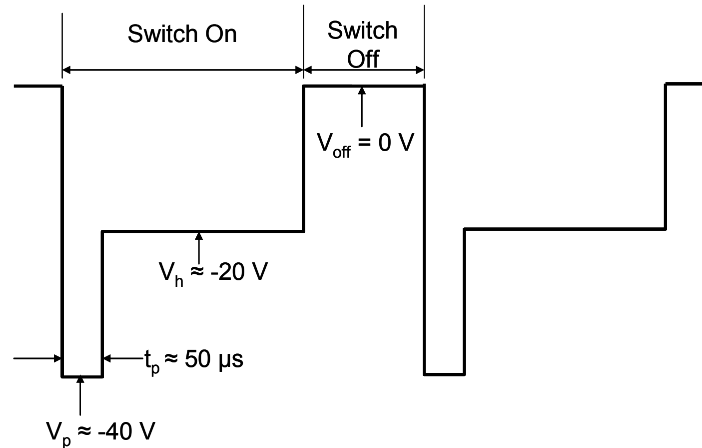

Figure 5 - Dual-pulse actuation waveform.

To estimate the improvement due to this waveform, the switch model of Equation (1) with values from Table 1 were used to evaluate dielectric charging. The shift in voltage due to charging was evaluated for three conditions, 1) a continuous DC voltage at -40 volts, 2) a 1 kHz, unipolar -40 volt square wave with a 50% duty cycle, and 3) a dual-pulse waveform with a 50 us actuation pulse at -40 volts and a holding voltage of -20 volts for 450 us. Simulations show that the 1 kHz square wave took 2.2x longer to charge, while the dual pulse waveform took 24.4x longer to charge to the same level. Measurements utilizing the dual-pulse waveform consistently show a significant improvement in longevity, supporting the calculations described.

In order to obtain high cycle counts in switch lifetime measurements, it is necessary to operate the switch as quickly as possible. With typical switching times of ~5-8 microseconds, operating at cycling frequencies above 50 kHz yields short on- or off-times, with most of the period spent in transit between the two states. These switches were operated at 60 kHz, with a cycle period of 16.7 µS. In this case, the effective duty cycle for on-time was on the order of 10%. Using Eqs (1) and (2), with the simulation techniques previously established[7], the impact of duty factor on dielectric charging can be quantified. Using the model data for silicon dioxide (J1: t=5 sec, $Qo=2\cdot10^{10}/cm^2$, Vo=16 volts, J2: t=52 sec, $Qo=6\cdot10^{10}/cm^2$, Vo=16 volts) , the saturated (infinite time) charge density as a function of duty factor for this dielectric film is modeled as shown in Figure 6. Operating at a 10% duty factor reduces the induced charge collected in the insulator by a factor (roughly linear) of 0.129. Reducing the duty cycle in this way also affords the opportunity to ascertain the saturated charge density of the insulator film, a very useful figure of merit.

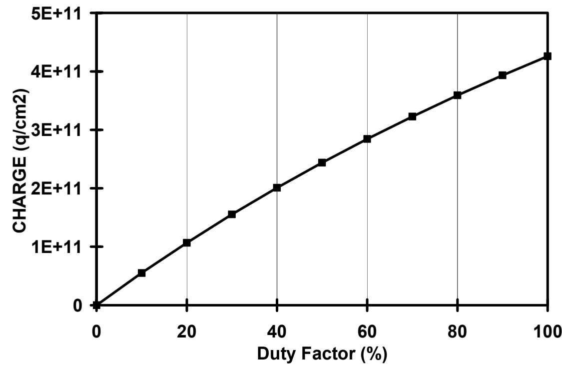

Figure 6 - Modeled maximum charge density as a function of on-time duty factor for a capacitive MEMS switch built with the dielectric of Table 1.

6. LIFETIME AND ACCELERATED TESTING

To life test an RF MEMS switch, the switch is repeatedly actuated until failure. The most effective means of accomplishing this is to apply a continuous RF signal and monitor the modulated signal caused by the actuation of the switch. This provides a real time, dynamic sensing of switch operation.

6.1 Lifetime testing with diagnostic monitoring

A test set used to lifetest and monitor a MEMS switch is shown in Figure 7. An HP 8350B sweep oscillator with an HP 83572B plug-in supplies a continuous 35 GHz signal at 5 mW of RF power. Meanwhile, an HP 33220A arbitrary wave generator followed by a Tabor Electronics 9100 high voltage amplifier creates the drive signal to actuate the switch. These RF and DC signals are multiplexed onto the RF line by a Picosecond Pulse Labs 5585 bias tee. These signals are applied to the device under test on a Cascade Microtech 11751HT thermal probe station through Cascade Infinity probes. The temperature of the sample is controlled by a Temptronic LM00550 temperature controller, while the environment of the device is controlled by dry air flowing through the test station microchamber. The output of the probe station ultimately feeds an HP R422A crystal detector for real time monitoring of switch actuation on a digital oscilloscope. The waveguide input of this detector serves as a high-pass filter to mitigate the impact of control voltage switching transients on the detector.

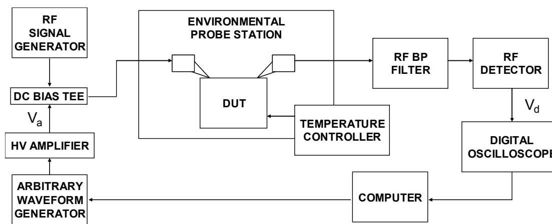

Figure 7 - Block diagram of MEMS lifetime test station.

This test technique has been extended to provide in-situ monitoring of switch operating parameters throughout the test. This is accomplished by switching between diagnostic and tactical waveforms during the test. The diagnostic waveform allows dynamic monitoring of electromechanical properties (pull-in and release voltages) and RF performance (on-capacitance and off-capacitance). Figure 8 demonstrates a typical operating curve for a MEMS capacitive switch obtained using this technique. The diagnostic waveform consists of a series of four ramped pulses of which have periods of 1 ms. The switch operating curve is generated by graphing the detected signal against the applied voltage. Both pull-in and release events are apparent from the abrupt changes in detector voltage. The magnitude of attenuation of the detector signal during actuation yields approximate information regarding the on-capacitance of the switch.

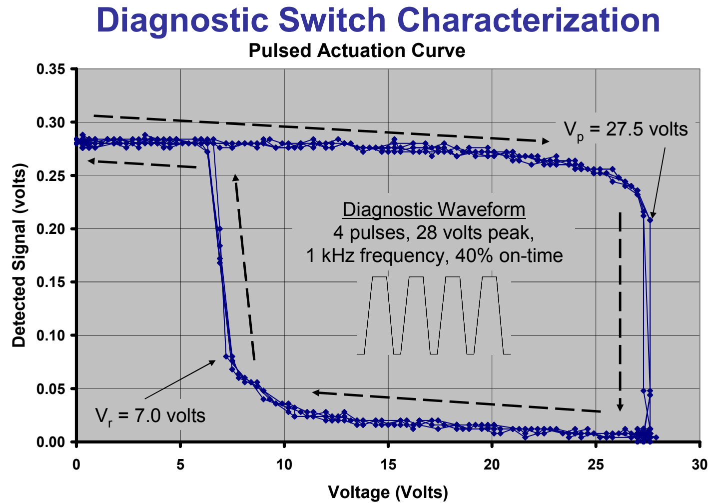

Figure 8 - Pulsed actuation curve used to obtain diagnostic information on switch operation.

Alternatively, the RF detector and signal source can be replaced with a Booton 5200 capacitance meter to dynamically measure capacitance at 1 MHz. A resulting switch operating curve (for a proximity switch) is shown in Figure 9. This type of curve quantifies the switch capacitance during operation.

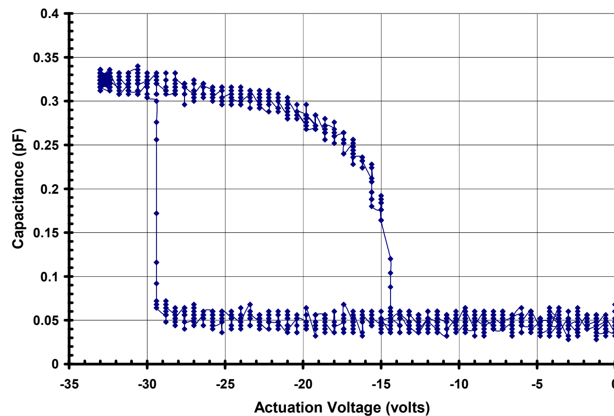

Figure 9 - Dynamic operating curve for the MEMS proximity switch.

By repeatedly measuring the dynamic performance of the switch during cycling, a view of the charging phenomena can be evaluated over time. This enables quantification of the charging (or determination that failures were for reasons other than charging) throughout the lifetest of the switch. Figure 10 is a graphical representation of the change in pull-in and release voltages (Vp and Vr, respectively) throughout the duration of a short life test of a proximity switch. This method is used to quantify charging behavior as well as function as in infant mortality test for extended life testing.

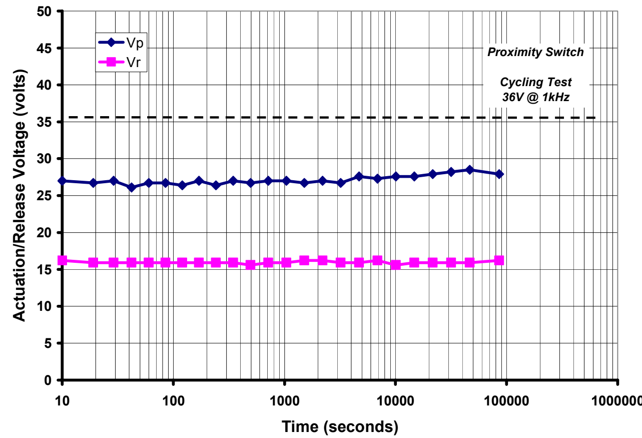

Figure 10 - Evolution of proximity switch operating characteristics (pull-in and release voltages) under cycling life test.

6.2 Accelerated testing with diagnostic monitoring

Accelerated dielectric charging within the switch is accomplished through the continuous application of DC voltage to the switch. A constant drive voltage, above the switch pull-in voltage, places the switch in the actuated state and provides a high electric field which continuously induces charges into the dielectric. At repeated time intervals, the waveform generator is signaled to apply the cycling (diagnostic) waveform to the switch to assess its electromechanical and RF performance. Afterwards, the drive voltage is switched back to the constant DC signal. This results in the measurement of the worst-case dielectric charging within the switch insulator.

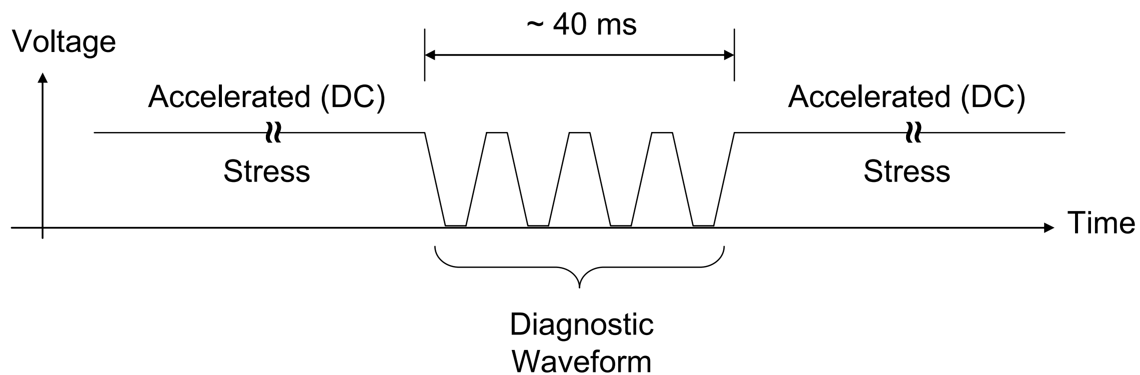

Figure 11 - Graphical depiction of a portion of the accelerated life time test.

Figure 12 demonstrates the shift in pull-in and release voltages during the accelerating testing of the full capacitive switch. This technique is enormously useful in characterizing the full extent of dielectric charging, and provides a data point for estimating the amount of charging that a switch will experience in actual operation. The techniques discussed in Section 5.3 provide a means for estimating the scaling of charging with voltage and time.

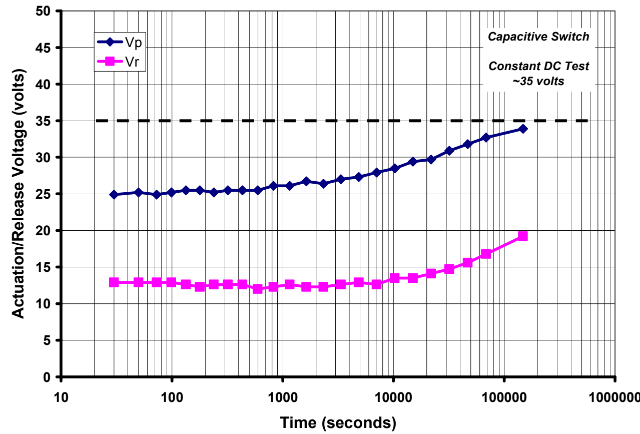

Figure 12 - Evolution of capacitive switch operating characteristics (pull-in and release voltages) under accelerated life test.

7. HIGH-CYCLE SWITCH TESTING

Beyond the impact of dielectric charging, it is important to know whether there are other mechanical failure or drift mechanisms at work during extended periods of cycling. For this purpose, cycling switches at high repetition rates to accumulate large cycle counts are useful. To this end, a switch as described above, was operated at -30 volts bias using a trapezoidal waveform at a repetition frequency of 60 kHz. The effective duty cycle of the switch was 10%. At this rate, the switch cycled at 216 million cycles/hr. The switch was run for a total of 476 hours without failure, accumulating a total of 102.8 billion cycles[8]. During the course of this test, snapshots of the high speed (60 kHz) operating waveforms were recorded. In addition, operation was slowed at regular intervals to obtain slow-speed (1 kHz) operating curves. The equipment and procedures for these characterizations are given above. The high-speed waveforms yielded information regarding the on- and off-states of the switch over the duration of the test, while the slow-speed curves yielded diagnostic information regarding changes in pull-in and release voltages.

7.1 Measurements

From the high-speed operating data, points were accumulated at the minimum and maximum (fully up and fully down) RF output powers to determine if there was drift in the RF performance of the device over the duration of the test. As can be seen in Figure 13, the off-state (contact open) performance of the switch was very stable over time. Though there was some drift in the on-state (contact closed) detector signal over time, it is hard to quantify how much is generator or detector drift over the three weeks of testing. Qualitatively, there was no significant degradation of the switch after accumulating the 100 billion cycles.

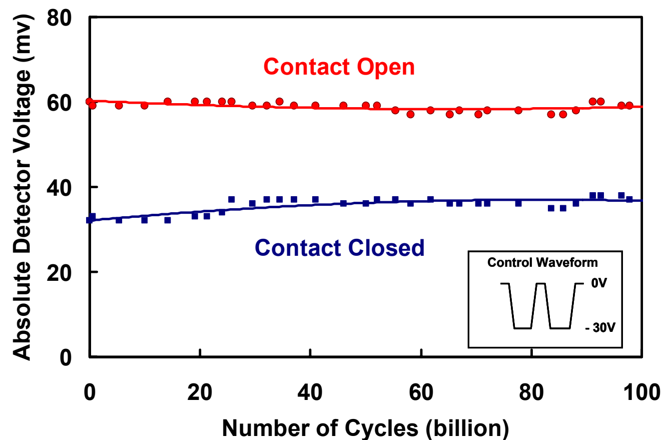

Figure 13 - Isolation and insertion performance of switch during cycling.

From the slow-speed operating curves, data points were accumulated to track the change in pull-in and release voltages. This provided information regarding the electromechanical performance and dielectric charging of the switch. Figure 14 displays the extracted voltages as a function of accumulated cycles.

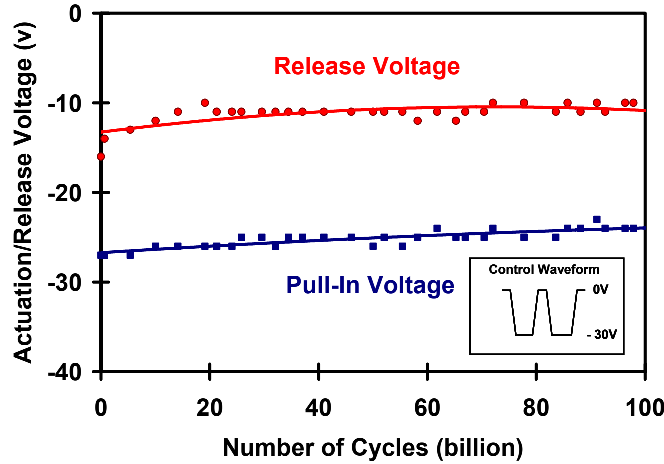

Figure 14 - Diagnostic evaluation of switch operating parameters over cycle lifetime.

As can be seen from the graph, the change in pull-in and release voltages were monotonic over time (cycles). The total shift in pull-in voltage was 3 volts, while the total shift in release voltage was approximately 5 volts. Changes in pull-in voltage are likely a better metric of dielectric charging, as release voltages are also impacted by surface conditions of the switch[9].

7.2 Analysis

The amount of charge accumulated during the 100 billion cycle test can be estimated as

$$\Delta V = hQ / \varepsilon_R \varepsilon_O$$

Where h is the effective height of a sheet of charge of density Q, within an insulator having a relative dielectric constant of ε_R. With h being approximately half the thickness of the dielectric film[2], 1400A, this yields a saturated charge density of $6.5 \cdot 10^{11}$ carriers/cm^2.

Accounting for the dielectric fill factor and the operating duty factor, this equates to a maximum saturated carrier density of $2 \cdot 10^{13}$ carriers/cm^2 for a solid film of sputtered silicon dioxide operated under 100% duty cycle at -30 volts. This becomes a useful film figure-of-merit for estimating the performance of switches with differing fill factors or operating conditions.

8. SUMMARY

Progress in the characterization and modeling of dielectric charging in MEMS capacitive switches is providing a much improved understanding of this failure mechanism. New in-situ diagnostic testing methods for cycling and accelerated testing provide insights into the evolution of dielectric charging and its impact during the lifetime of the switch. These innovations provide significantly better tools for designing MEMS capacitive switches for increased longevity. These techniques have been utilized to show that a switch capable of order-of-magnitude impedance changes can operate for extended periods, greater than 100 billion cycles, without charging-induced failure. It also demonstrates that the underlying mechanics of MEMS devices are robust and that the detrimental effects of dielectric charging can be managed. Application of these tools and techniques is expected to continue improving the reliability and robustness of this critical technology for DOD applications.

ACKNOWLEDGEMENTS

The authors appreciate the sponsorship of the Defense Advanced Research Projects Agency under Contract F33615-03-C-7003, for which this work was performed.

REFERENCES

[1] Z.J. Yao, S. Chen, S. Eshelman, D. Denniston, and C. Goldsmith, "Micromachined low-loss microwave switches," *Journal of Microelectromechanical Systems* **8(2)**, 129-134 (1999).

[2] X.B. Yuan, J.C.M. Hwang, D. Forehand, and C.L. Goldsmith, "Modeling and Characterization of Dielectric-Charging Effects in RF MEMS Capacitive Switches," *2005 IEEE Int. Microwave Symp. Dig.* paper WE3B-3, (2005).

[3] C. Goldsmith, D. Forehand, X.B. Yuan, and J. Hwang, "Tailoring Capacitive Switch Technology for Reliable Operation," *2006 Govt Microcircuit Applications and Critical Tech Conf*, 1-4 (2006).

[4] C. Goldsmith, J. Ehmke, A. Malczewski, B. Pillans, S. Eshelman, Z. Yao, J. Brank, and M. Eberly, "Lifetime Characterization Of Capacitive RF MEMS Switches," *2001 IEEE Int. Microwave Symp. Dig.* **1**, 227-230 (2001).

[5] C.L. Goldsmith, "Proximity Micromechanical Systems," *United States Patent 6,608,268*, issued August 19, 2003.

[6] P. Blondy, A. Crunteanu, C. Champeaux, A. Catherinot, P. Tristant, O. Vendier, J.L. Cazaux, and L. Marchand, "Dielectric Less Capacitive MEMS Switches," *2004 IEEE Int. Microwave Symp. Dig.*, 573-576 (2004).

[7] X.B. Yuan, Z. Peng, J.C.M. Hwang, D. Forehand, and C.L. Goldsmith, "A transient SPICE model for dielectric-charging effects in RF MEMS capacitive switches," *IEEE Trans Elect Dev* **53(10)**, 2640-2648 (2006).

[8] C.L. Goldsmith, D.I. Forehand, Z. Peng, J.C.M. Hwang, and J.L. Ebel, "High-Cycle Life Testing of RF MEMS Switches," 2007 IEEE Intl Microwave Symp Dig., 1805-1808 (2007).

[9] J.F. Kucko, J.C. Petrosky, J.R. Reid, and Y.K. Yeo, "Non-Charge Related Mechanism Affecting Capacitive MEMS Switch Lifetime," *IEEE Microwave Wireless Comp. Lett*. **16(3)**, 140-142 (2006).